Pergamon

Int. J. Heat Mass Transfer. Vol. 39, No. 6, pp. 1175–1181, 1996

0017-9310/96 $15.00+0.00

0017-9310(95)00209-X

Maximum power from fluid flow

ADRIAN BEJAN

Department of Mechanical Engineering and Materials Science, Duke University, Box 90300, Durham, NC 27708-0300, U.S.A.

(*Received* 26 *October* 1994 *and in final form* 6 *June* 1995)

Abstract—The heat transfer principle of power maximization in power plants with heat transfer irreversibilities is extended to fluid flow. It is shown that when a stream flows between two pressure reservoirs ($P_1 > P_2$) across linear flow resistances, a piston delivers maximum power when the pressure difference across its faces is $(P_1 - P_2)/2$. The energy conversion efficiency at maximum power is $\eta_{max} = (1/2)(1 - P_2/P_1)$, as an analog to the efficiency for maximum power in power plants, $\eta_{max} = 1 - (T_2/T_1)^{1/2}$. These results are generalized to fluid flow with nonlinear relations of pressure drop vs flow rate. Depending on overall size constraints, the power delivery can be further maximized by balancing the flow resistances upstream and downstream of the piston. The paper concludes with applications to steady-flow shaft-power components. It is shown that turbines can be optimized for maximum power output by selecting the inlet or outlet pressure drop, or the flowrate. Compressors and pumps do not have a power input minimum with respect to pressure drop or flowrate.

1. INTRODUCTION

In this paper I consider the fundamental thermodynamic problem of how to extract maximum instantaneous power from a fluid flow driven from a high pressure reservoir (P_1) to a low pressure reservoir (P_2). The corresponding maximum power problem of heat engines operating with thermal resistances between two temperature reservoirs has been treated in great detail in the literature. The work on maximum-power heat engines began with Novikov [1], Chambadal [2] and Curzon and Ahlborn [3], and generated a voluminous literature that was reviewed on several occasions, most recently in the book by Bejan [4]. The method of combining heat transfer with thermodynamics is more general, with a wide range of applications in addition to power plant optimization [5]. The method is known as thermodynamic optimization or entropy generation minimization.

There is an important analogy between the irreversibility of heat transfer across a finite temperature difference (thermal resistance) and the irreversibility of fluid flow across a finite pressure drop (fluid resistance). This analogy was stressed in ref. [5], pp. 35–38, and is responsible for the competition between heat transfer and fluid flow in the minimization of the entropy generation rate associated with convection heat transfer. The analogy was also exploited by Radcenco [6] in a series of component optimization applications (turbines, compressors) that will be analyzed in Section 6.

The objectives of the present paper are:

(i) to extend to the field of fluid power conversion the thermodynamic optimization principles developed for thermal power conversion,

(ii) to show the analogy between the fluid and thermal maximum power designs,

(iii) to illustrate the physical meaning of the heat engine power maximum by using the purely mechanical analog and language of the flow driven between two pressure reservoirs and

(iv) to illustrate the practical meaning of the fluid power maximum by optimizing actual steady-flow shaft-work components such as turbines, compressors and pumps.

2. EXTRACTION OF POWER FROM FLUID FLOW BETWEEN TWO PRESSURE RESERVOIRS

Consider the piston and cylinder apparatus shown in Fig. 1. The piston moves with friction under the influence of the pressure difference $P_{1C} - P_{2C}$ maintained across its two faces. The instantaneous power delivered by the piston to an external system is

$$\dot{W} = (P_{1C} - P_{2C})AV - A_f \frac{\mu}{\delta} V \quad (1)$$

where A, A_f and V are the piston frontal area, the lateral (friction) area, and the instantaneous speed. The ratio μ/δ accounts for Couette flow in the relative motion gap of thickness δ, where μ is the viscosity of the lubricant. The piston inertia is assumed negligible.

The working fluid experiences a pressure drop $(P_1 - P_{1C})$ as it is admitted from the resevoir P_1 to the chamber on the driven side of piston. Similarly, the fluid ejected from the chamber positioned on the driving side of the piston experiences another pressure drop, $(P_{2C} - P_2)$. By analogy with the simplest heat transfer model used in power maximization studies of thermal energy conversion (e.g. ref. [5], p. 146), we

NOMENCLATURE

a, b	dimensionless parameters, equation (32)
A	piston frontal area
A_f	lateral, friction area
c_p	specific heat at constant pressure
C	constant
D	overall thickness
D_1, D_2	channel spacings, Fig. 3(b)
L	overall length
L_1, L_2	duct lengths, Fig. 3(a)
$\dot{m}$	mass flow rate
n	exponent, equations (20) and (21)
P_1, P_2	pressure reservoirs
P_{1C}, P_{2C}	pressures across the piston
r_1, r_2	flow resistances, equations (20) and (21)
R_1, R_2	flow resistances, equations (2) and (3)
T_1, T_2	temperature reservoirs
T_{1C}, T_{2C}	temperatures across the reversible part of the heat engine, Fig. 2
UA	thermal conductance
V	piston velocity
V_0	piston velocity at zero power output
V_2	mean fluid velocity in the downstream duct, Fig. 3(a)
$\dot{W}$	power output, equation (1) and Fig. 2
x	relative channel spacing, equation (16)
y	dimensionless pressure drop, equation (32).

Greek symbols

δ	piston–cylinder gap thickness
ΔP_f	pressure difference due to piston–cylinder friction
$\Delta P_1, \Delta P_2$	pressure drops
η_c	compressor isentropic efficiency
η_{max}	efficiency at maximum power
η_{rev}	efficiency in the reversible limit
η_t'	turbine isentropic efficiency
$\eta_{II,max}$	second law efficiency at maximum power
μ	viscosity of lubricant.

assume that the pressure differences are proportional to the respective flow rates, which in turn are proportional to V:

$$P_1 - P_{1C} = R_1 V \tag{2}$$

$$P_{2C} - P_2 = R_2 V. \tag{3}$$

In these expressions R_1 and R_2 are the two instantaneous fluid resistances. The fluid is being assumed incompressible on both sides of the piston. The linear model (2, 3) is appropriate for laminar flow such as in capillary ducts for micromechanical energy converters. A model for higher Reynolds number flows is presented in Section 5.

The resevoir pressures P_1 and P_2 are fixed, however, P_{1C} and P_{2C} depend on the piston speed, which is the only degree of freedom in the operation of the mechanical energy conversion device shown in Fig. 1. The optimal speed for maximum instantaneous power delivery can be obtained by eliminating P_{1C} and V between equations (2, 3), substituting into equation (1), and solving $\partial \dot{W}/\partial P_{2C} = 0$. The result for the optimal downstream pressure is

$$P_{2C,opt} = \frac{P_1 + (1 + 2R_1/R_2)P_2 - \Delta P_f}{2(1 + R_1/R_2)} \tag{4}$$

where $\Delta P_f = A_f \mu/(A\delta)$ is the pressure drop due solely to piston–cylinder friction. The remaining parts of the maximum-power solution are obtained by substituting equation (4) back into equations (1)–(3):

$$P_{1C,opt} = \frac{P_2 + (1 + 2R_2/R_1)P_1 + \Delta P_f}{2(1 + R_2/R_1)} \tag{5}$$

$$V_{opt} = \frac{P_1 - P_2 - \Delta P_f}{2(R_1 + R_2)} \tag{6}$$

$$\dot{W}_{max} = \frac{A(P_1 - P_2 - \Delta P_f)^2}{4(R_1 + R_2)}. \tag{7}$$

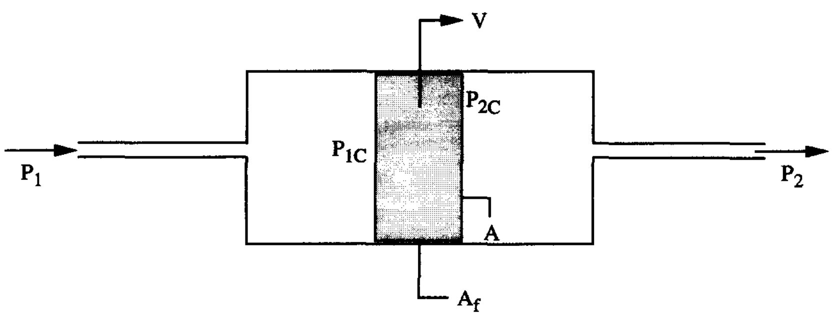

Fig. 1. Piston and cylinder apparatus for extracting mechanical power from the flow of a fluid between two pressure reservoirs.

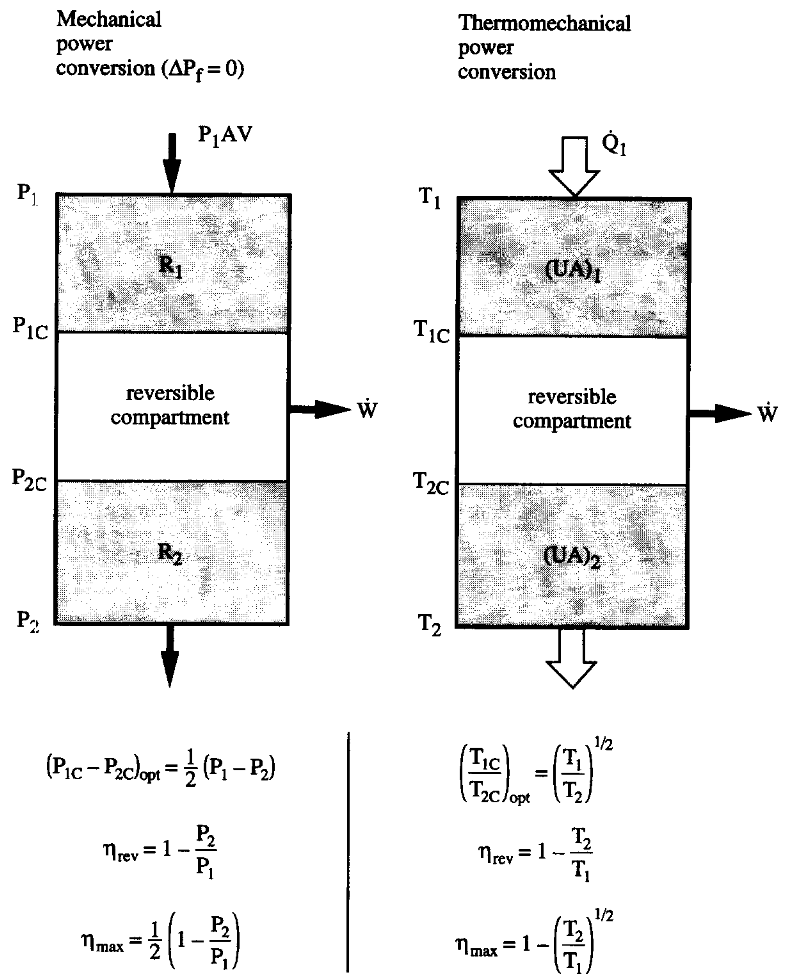

Fig. 2. The analogy between the maximum power conditions for fluid power conversion vs thermal power conversion.

One way to interpret the maximum power condition is to calculate the pressure difference across the piston, and compare it with the overall pressure difference:

$$(P_{1C}-P_{2C})_{opt} = \tfrac{1}{2}(P_1-P_2+\Delta P_f). \tag{8}$$

We learn that in the limit of negligible piston friction, the pressure difference across the piston must be exactly half of the reservoir-to-reservoir pressure difference. There is symmetry between this result and the corresponding result for a power plant sandwiched between two thermal resistances (Fig. 2): pressure differences play the role of absolute temperature ratios. Furthermore, 1/2 appears as a factor in equation (8) and as an exponent in the case of a thermal power plant optimized for maximum power.

Another way is to compare the optimal instantaneous speed (V_{opt}) with the piston speed in the limit of zero power delivery (V_0). The latter is obtained by combining $\dot{W} = 0$ with equations (1)–(3)

$$V_0 = \frac{P_1-P_2-\Delta P_f}{R_1+R_2}. \tag{9}$$

Equations (6) and (9) show that the piston speed at maximum power is exactly half of the piston speed at zero power, $V_{opt} = V_0/2$, regardless of whether piston friction is negligible.

3. THE CONVERSION EFFICIENCY AT MAXIMUM POWER

The work transfer rate received from the P_1 reservoir is P_1AV. This quantity is analogous to the heat transfer rate $\dot{Q}_1$ of the corresponding heat engine model, Fig. 2. In the reversible limit ($\Delta P_f = 0$, $R_1 = 0$, $R_2 = 0$), the mechanical power drawn from P_1AV and delivered by the moving piston is only $\dot{W}_{rev} = (P_1-P_2)AV$, because the portion P_2AV is being absorbed by the P_2 reservoir. The power conversion efficiency in the reversible limit is

$$\eta_{rev} = \frac{\dot{W}_{rev}}{P_1AV} = 1-\frac{P_2}{P_1}. \tag{10}$$

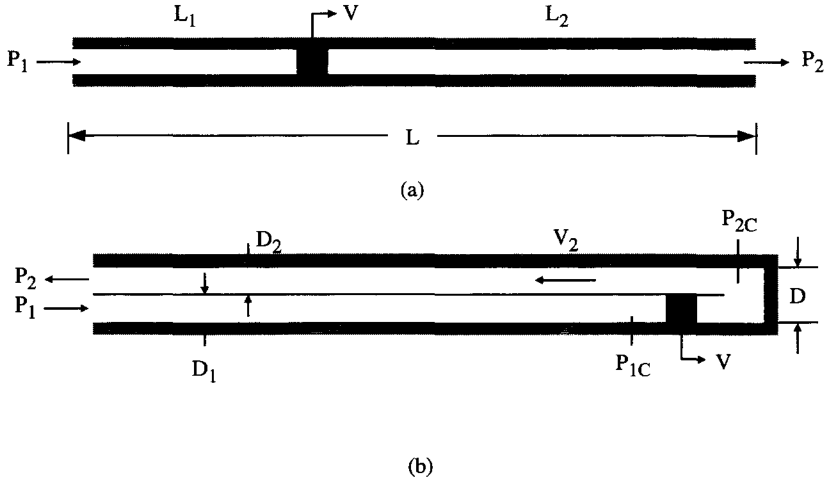

Fig. 3. Examples of overall size constraints: (a) fixed total length and pressure reservoirs on opposite sides of the piston; (b) fixed total length and thickness, and pressure reservoirs on the same side of the piston.

The symmetry between η_{rev} and the Carnot efficiency of a heat engine $(1-T_2/T_1)$ is evident.

The conversion efficiency of the device of Fig. 1 under conditions of maximum power delivery is

$$\eta_{max} = \frac{\dot{W}_{max}}{P_1 A V_{opt}} \tag{11}$$

or, after using equations (6) and (7)

$$\eta_{max} = \frac{1}{2}\left(1 - \frac{P_2}{P_1} - \frac{\Delta P_f}{P_1}\right). \tag{12}$$

The maximum-power efficiency is exactly half of the reversible-limit efficiency when piston friction is negligible. This case is compared in Fig. 2 with the maximum-power efficiency of a heat engine, $1-(T_2/T_1)^{1/2}$. Again, as in the first line of the table of Fig. 2, the 1/2 factor of the formula for fluid power conversion becomes an exponent in the formula for thermal power conversion. In general, the effect of increasing piston friction is to shift the maximum power design toward lower η_{max}, $\dot{W}_{max}$ and V_{opt}.

4. OVERALL SIZE CONSTRAINTS

Another issue that relates the two columns of Fig. 2 concerns the overall size constraint that must be faced by the actual device. On the heat engine side of the figure, this issue has been studied extensively for the purpose of determining the optimal allocation of a finite heat transfer area (or thermal conductance) between the two heat exchangers [7, 8]. In the case of the general fluid power converter shown in Fig. 1, the impact of the overall size constraint depends on the shape (layout) of the system.

To illustrate this point, consider the long and thin tube of length L shown in Fig. 3(a), and assume that $\Delta P_f = 0$. The instantaneous position of the piston divides L into two sections, the driving fluid column L_1, and the driven column L_2. The corresponding flow resistances of these two sections are

$$R_1 = CL_1 \quad \text{and} \quad R_2 = CL_2 \tag{13}$$

where C is a Hagen–Poiseuille flow constant that depends on viscosity and tube diameter. The important observation is that C is the same on both sides of the piston, which means that

$$R_1 + R_2 = CL \quad \text{(constant)}. \tag{14}$$

In conclusion, equations (6) and (7) show that V_{opt} and $\dot{W}_{max}$ do not depend on the position occupied by the piston along L. In other words, in the device of Fig. 3(a) there is no optimum with respect to the way in which L is divided into L_1 and L_2. The absence of such an optimum distinguishes the mechanical device of Fig. 3(a) from the heat engine model optimized in refs. [7] and [8].

In the second example, Fig. 3(b), we continue to assume that $\Delta P_f = 0$. This time the two pressure reservoirs are positioned to the left of the piston, while the two fluid columns are oriented in counterflow. Let us assume that the overall size of the device is fixed, $L \times D$, and that the fluid columns flow through narrow parallel-plate channels of spacing D_1 and, respectively, D_2. The overall thickness constraint

$$D_1 + D_2 = D \quad \text{(constant)} \tag{15}$$

makes the relative thickness x of one channel the only degree of freedom

$$D_1 = xD \quad D_2 = (1-x)D. \tag{16}$$

Assuming that the piston is close to the end-turn region, and that the flow is of the Hagen–Poiseuille type in both channels, we have

$$P_1 - P_{1C} = \frac{12\mu L}{D_1^2} V \tag{17}$$

$$P_{2C}-P_2=\frac{12\mu L}{D_2^2}V_2 \quad (18)$$

where V_2 is the mean velocity in the D_2 channel. Mass conservation requires $VD_1 = V_2D_2$; after comparing equations (17) and (18) with equations (2) and (3) we conclude that the flow resistances are

$$R_1=\frac{12\mu L}{D_1^2} \quad \text{and} \quad R_2=\frac{12\mu LD_1}{D_2^3}. \quad (19)$$

To further maximize $\dot{W}_{max}$ of equation (7) we must minimize (R_1+R_2), which is equivalent to minimizing the function $(D_1^{-2}+D_1/D_2^3)$, or $[x^{-2}+x/(1-x)^3]$. The optimal relative spacing is $x_{opt} = 0.454$, which means that the downstream channel should be 20% wider than the upstream channel. The optimal spacings D_1 and D_2 are not equal because the geometry of Fig. 3(b) is not symmetric with respect to the two channels (the piston is inside *one* of the channels, i.e. the D_1 channel).

5. NONLINEAR FLOW RESISTANCE RELATIONS

The power maximization principles discussed until now also apply at higher Reynolds numbers, where the linear flow resistance model, equations (2) and (3) is replaced by nonlinear relations. A general model that relates the pressure drops to the instantaneous flowrate is

$$P_1-P_{1C}=r_1V^n \quad (20)$$

$$P_{2C}-P_2=r_2V^n \quad (21)$$

where $1 \lesssim n \lesssim 2$, and (r_1, r_2) are constant coefficients that depend on duct geometry and fluid properties. As in turbulent flow through a duct with rough walls, through an orifice [9], or through a porous medium [10], the n exponent increases as the Reynolds number increases. Clearly, the $n = 1$ limit represents the regime analyzed in Sections 2–4.

Let us assume that at high Reynolds numbers the piston friction term is negligible on the right-hand side of equation (1). Combining equation (1) with equations (20) and (21) we find that the operation at maximum power is described by

$$P_{1C,opt}=\frac{P_1(1+2r_2/r_1)-P_2[n-2+(n-1)r_1/r_2]}{2(1+r_2/r_1)} \quad (22)$$

$$P_{2C,opt}=\frac{P_1+P_2[n+(n+1)r_1/r_2]}{2(1+r_1/r_2)} \quad (23)$$

$$V_{opt}=\left(\frac{P_1+P_2[(n-2)+(n-1)r_1/r_2]}{2(r_1+r_2)}\right)^{1/n} \quad (24)$$

$$(P_{1C}-P_{2C})_{opt}=\frac{1}{2}\left\{P_1-P_2\left[n+(n-1)\frac{r_1}{r_2}\right]\right\}. \quad (25)$$

The maximum power output can be calculated using $\dot{W}_{max} = (P_{1C}-P_{2C})_{opt}AV_{opt}$. The efficiency at maximum power is given by

$$\eta_{max}=\frac{\dot{W}_{max}}{P_1AV_{opt}}=\frac{1}{2}\left\{1-\frac{P_2}{P_1}\left[n+(n-1)\frac{r_1}{r_2}\right]\right\} \quad (26)$$

which shows that η_{max} decreases as n increases. Finally, equation (26) can be restated as a second law efficiency at maximum power,

$$\eta_{II,max}=\frac{\eta_{max}}{\eta_{rev}}=\frac{1}{2}\left[1-(n-1)\left(1+\frac{r_1}{r_2}\right)\frac{P_2}{P_1-P_2}\right]. \quad (27)$$

In the $n = 1$ limit the second law efficiency is equal to 1/2, which can also be seen by dividing equation (12) by equation (10) when $\Delta P_f = 0$. The second law efficiency drops below 1/2 as n becomes greater than 1.

6. APPLICATIONS

The maximization of power extraction from fluid flow has potential applications in the optimization of power plants. This opportunity was pointed out recently by Radcenco [6], who analyzed the effect of finite inlet and outlet flow resistances in internal combustion engines, gas turbine power plants and reciprocating compressors and expanders, by assuming linear and nonlinear pressure drop relations and isentropic expansion and compression. In this section we illustrate these research opportunities by extending the simple model of Fig. 1 to steady-state shaft-work machines such as turbines, compressors and pumps.

6.1. *Turbine*

Consider the adiabatic steady flow turbine shown in Fig. 4. An ideal gas of flow rate $\dot{m}$ expands from P_1 to P_2, as shown on the attached *T–s* diagram. The stream experiences the pressure drop ΔP_1 as it is ducted and distributed to the first turbine stage. It then expands through the turbine stage (or sequence of stages), which has the isentropic efficiency η_t. Note that to account for the nonisentropic expansion ($\eta_t < 1$) in Fig. 4 is equivalent to accounting for piston friction (ΔP_f) in Fig. 1. The final pressure drop, ΔP_2, is due to the discharge and ducting of the stream to the next component in the power plant (cooler, or condenser). We continue to assume that the relation between pressure drop and flow rate is nonlinear as in equations (20) and (21),

$$\Delta P_1=r_1\dot{m}^n \quad (28)$$

$$\Delta P_2=r_2\dot{m}^n. \quad (29)$$

The power output of the turbine

$$\dot{W}=\eta_t\dot{m}c_pT_1\left[1-\left(\frac{P_2+\Delta P_2}{P_1-\Delta P_1}\right)^{R/c_p}\right] \quad (30)$$

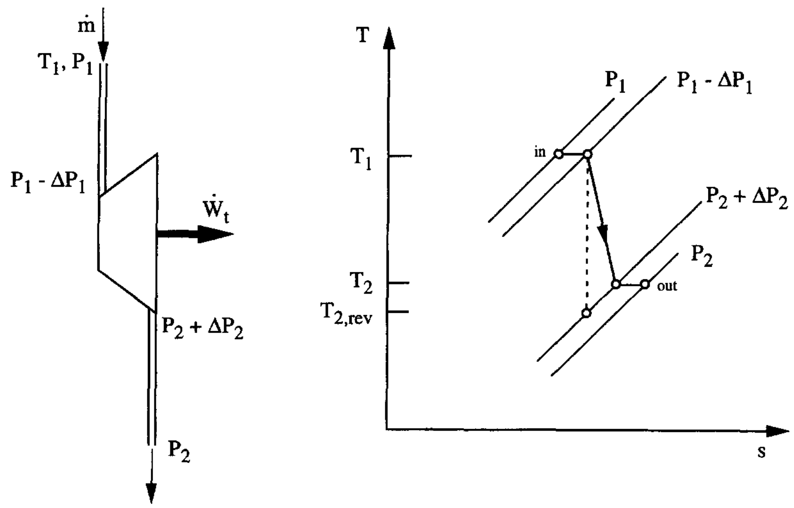

Fig. 4. Steady flow turbine with entrance and exit pressure drops.

can be expressed as a function of ΔP_1 by eliminating ΔP_2 and $\dot{m}$ between equations (28), (29) and (30). If we further assume that $\Delta P_1 \ll P_1$ and $\Delta P_2 \ll P_2$, the resulting expression is

$$\dot{W} = \eta_t c_p T_1 \left(\frac{P_1}{r_1}\right)^{1/n} y^{1/n}(1-b-aby) \quad (31)$$

where

$$y = \frac{\Delta P_1}{P_1} \quad a = \frac{R}{c_p}\left(1+\frac{r_2 P_1}{r_1 P_2}\right) \quad b = \left(\frac{P_2}{P_1}\right)^{R/c_p}. \quad (32)$$

Solving $\partial \dot{W}/\partial y = 0$ we obtain the condition for operation at maximum power

$$y_{opt} = \frac{\Delta P_{1,opt}}{P_1} = \frac{1-b}{ab(1+n)} \ll 1 \quad (33)$$

$$\dot{W}_{max} = \eta_t c_p T_1 \left(\frac{P_1}{r_1}\right)^{1/n} \frac{n}{(ab)^{1/n}} \left(\frac{1-b}{1+n}\right)^{1+1/n} \quad (34)$$

$$\dot{m}_{opt} = \left(\frac{\Delta P_{1,opt}}{r_1}\right)^{1/n} \quad \Delta P_{2,opt} = \frac{r_2}{r_1}\Delta P_{1,opt}. \quad (35)$$

It is instructive to compare the maximum power output (34) for finite r_1 and r_2 with the power at the same flowrate ($\dot{m}_{opt}$) in the limit of zero pressure drops ($r_1 = r_2 = 0$), namely

$$\dot{W}_{r_1=r_2=0} = \eta_t \dot{m}_{opt} c_p T_1 \left[1-\left(\frac{P_2}{P_1}\right)^{R/c_p}\right]. \quad (36)$$

The ratio

$$\frac{\dot{W}_{max}}{\dot{W}_{r_1=r_2=0}} = \frac{n}{1+n} < 1 \quad (37)$$

is equal to 1/2 when the pressure drop relations, equations (28) and (29), are linear ($n = 1$). The 1/2 value reminds us of a similar result obtained in equation (12) for linear pressure drop relations.

6.2. *Compressor*

The analysis of the ideal-gas compressor with inlet and outlet pressure drops can be carried out similarly by using Fig. 5 and the pressure drop models (28) and (29). The isentropic efficiency of the compression stage (or sequence of stages) is η_c. The compressor power input

$$\dot{W}_c = \frac{1}{\eta_c}\dot{m} c_p T_1 \left[\left(\frac{P_2+\Delta P_2}{P_1-\Delta P_1}\right)^{R/c_p} - 1\right] \quad (38)$$

can be reduced to

$$\dot{W}_c = \frac{1}{\eta_c} c_p T_1 \left(\frac{P_1}{r_1}\right)^{1/n} y^{1/n}[b-1+aby] \quad (39)$$

where $\Delta P_1 \ll P_1$, $\Delta P_2 \ll P_2$ and (y, a, b) are given by equations (32). Note that this time b is greater than 1, and that $\dot{W}_c$ does not have a minimum with respect to y when y is positive. The absence of an optimal ΔP_1, or an optimal pressure ratio across the 'inner compartment' of the compressor model is analogous to the absence of an optimal temperature ratio across the inner (reversible) compartment of a refrigerator with warm and cold thermal resistances [11–13]. The common feature of compressors and refrigerators is that they require power inputs. In contrast to these, turbines and power plants are producers of power and have optimal pressure and temperature ratios.

6.3. *Pump*

Conclusions similar to those reached for the compressor are obtained in an analysis of a steady flow pump that operates on an incompressible fluid. When the finite intake and discharge flow resistances are taken into account, it is found that the pump power requirement increases monotonically with the pressure drops, or with the flow rate.

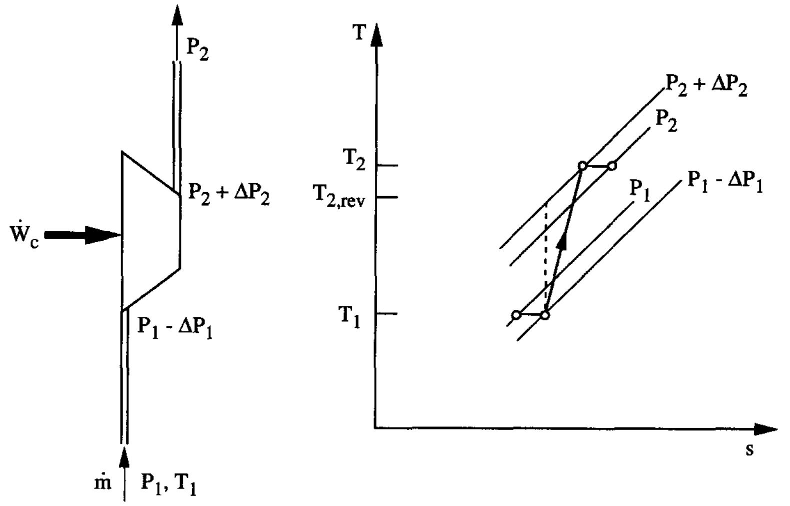

Fig. 5. Steady flow compressor with entrance and exit pressure drops.

6.4. *Overall size constraints*

The turbine power output $\dot{W}_{max}$ of equation (34) may be maximized once more with respect to the way in which the flow resistances r_1 and r_2 are balanced in a constraint dictated by overall size considerations. The same may apply to the compressor power input of equation (38). For example, Radcenco [6] fixed the sum of the cross-sectional areas of the intake and discharge valves of a reciprocating compressor and found the optimal ratio of the two areas.

7. CONCLUSIONS

The main conclusion of the work presented in this paper is that the power extracted from a flow can be maximized by selecting the optimal flow rate, or optimal pressure drops upstream and downstream of the actual work-producing device, Fig. 1. When the piston works with negligible friction, the conversion efficiency at maximum power is $(1-P_2/P_1)/2$. This result illustrates most succinctly the analogy between maximum power from fluid flow and maximum power from heat flow, Fig. 2.

The practical implications of the fluid flow power maximum were explored in Sections 4–6. Depending on the geometric layout and size of the overall system, it may be possible to increase the power output by balancing the inlet and outlet flow resistances. The applications of the maximum power principle to turbines, compressors and pumps (Section 6) and Radcenco's work [6] illustrate important research opportunities that deserve to be addressed in future studies.

Acknowledgements—This research was supported by the National Science Foundation. Professor V. Radcenco's comments on the original draft are very much appreciated.

REFERENCES

1. I. I. Novikov, The efficiency of atomic power stations, *J. Nuclear Energy II* **7**, 125–128 (1958); translated from *Atomnaya Energiya* **3** (11), 409 (1957).
2. P. Chambadal, *Les Centrales Nucleaires*, pp. 41–58. Armand Colin, Paris (1957).
3. F. L. Curzon and B. Ahlborn, Efficiency of a Carnot engine at maximum power output, *Am J. Phys.* **43,** 22–24 (1975).
4. A. Bejan, *Entropy Generation Minimization*. CRC Press, Boca Raton, FL (1996).
5. A. Bejan, *Entropy Generation through Heat and Fluid Flow*. Wiley, New York (1982).
6. V. Radcenco, *Generalized Thermodynamics*. Editura Tehnica, Bucharest (1994).
7. A. Bejan, Theory of heat transfer-irreversible power plants, *Int. J. Heat Mass Transfer* **31,** 1211–1218 (1988).
8. A. Bejan, *Advanced Engineering Thermodynamics*, pp. 409–411. Wiley, New York (1988).
9. I. E. Idelchik, *Handbook of Hydraulic Resistance* (3rd edn). CRC Press, Boca Raton, FL (1993).
10. D. A. Nield and A. Bejan, *Convection in Porous Media*. Springer, New York (1992).
11. A. Bejan, Theory of heat transfer-irreversible refrigeration plants, *Int. J. Heat Mass Transfer* **32,** 1631–1639 (1989).
12. S. A. Klein, Design considerations for refrigeration cycles, *Int. J. Refrig.* **15,** 181–185 (1992).
13. A. Bejan, Power and refrigeration plants for minimum heat exchanger inventory, *J. Energy Res. Technol.* **115,** 148–150 (1993).